

Evolution of discrete symmetries

Peter Schmelcher*

*Zentrum für Optische Quantentechnologien, Universität Hamburg, Luruper Chaussee 149, 22761 Hamburg, Germany
and The Hamburg Centre for Ultrafast Imaging, Universität Hamburg, Luruper Chaussee 149, 22761 Hamburg, Germany*

(Received 27 March 2023; accepted 5 October 2023; published 25 October 2023)

Symmetries are known to dictate important physical properties and can be used as a design principle in particular in wave physics, including wave structures and the resulting propagation dynamics. Local symmetries, in the sense of a symmetry that holds only in a finite domain of space, can be either the result of a self-organization process or a structural ingredient into a synthetically prepared physical system. Applying local symmetry operations to extend a given finite chain we show that the resulting one-dimensional lattice consists of a transient followed by a subsequent periodic behavior. Due to the fact that, by construction, the implanted local symmetries strongly overlap the resulting lattice possesses a dense skeleton of such symmetries. We prove this behavior on the basis of a class of local symmetry operations allowing us to conclude upon the “asymptotic” properties such as the final period, decomposition of the unit cell and the length and appearance of the transient. As an example case, we explore the corresponding tight-binding Hamiltonians. Their energy eigenvalue spectra and eigenstates are analyzed in some detail, showing in particular the strong variability of the localization properties of the eigenstates due to the presence of a plethora of local symmetries.

DOI: [10.1103/PhysRevE.108.044141](https://doi.org/10.1103/PhysRevE.108.044141)**I. INTRODUCTION**

Symmetries play a prominent role in many branches of physics. They represent a cornerstone both for the analysis and design of physical systems. Knowing the underlying symmetries of a setup under investigation allows us to predict certain symmetry-related properties without solving explicitly the corresponding equations of motion. The group theoretical description and classification of symmetries [1,2], be it discrete or continuous ones, provides us with, e.g., the parity of eigenstates or their rotational quantum numbers and multiplet structure and resulting the selection rules for their electromagnetic transitions in atoms, molecules, or bulk systems [3–5]. The typical and widely accepted situation assumes that a certain spatial symmetry holds for all of the space covered by the physical system under investigation, in short, it represents a global symmetry. The rotational symmetry of atoms, the point group symmetries of molecules, and the translation group symmetries of crystals all belong to this case. This is, however, by far not the most general structural behavior and many more complex but still geometrically appealing physical systems do not possess any global symmetry. One prominent example are quasicrystals [6–8] which generically do not possess any global symmetry but are governed by a plethora of local symmetries arranged in a quasiperiodic manner [9,10]. Here the notion of a local symmetry refers to the situation where a symmetry holds only on a limited subdomain of the domain of definition of a system. Quasicrystals represent one class of systems on the rich transition route from

periodicity to disorder and are nowadays of major importance in material science and technology [11,12].

More recently the concept of local symmetries has been further developed and applied to reveal a number of physical properties and phenomena. Breaking, e.g., the symmetry of a crystalline translation group and retaining only a local symmetry has been shown to lead to constants of motion which represent nonlocal currents that generalize the Bloch theorem for periodic crystals [13]. Multiple local symmetries can be combined to provide setups that are characterized by so-called nongapped or gapped local symmetries, where the gap refers to the space between the appearance of local symmetries, or systems with complete local symmetries for which local symmetries cover the setup completely. Applications to wave systems of acoustic [14] or electromagnetic [15] origin have shown that perfectly transmitting resonances can be designed based on sum rules of the nonlocal currents [16] which can also be used to detect local order via the analysis of the wave field. Indeed, the nonlocal currents fulfill generalized continuity equations in the framework of both the discrete [17] and the continuous theory [18]. A corresponding computational approach to efficiently handle locally symmetric wave systems has been developed in Ref. [19]. Remarkably in Ref. [20] it has been shown that the presence of local reflection symmetries in a one-dimensional finite and disordered chain severely impacts wave localization and transport. Due to the local symmetries correlations are imprinted into the wave field and specifically the corresponding transfer can be significantly enhanced if the occurring local symmetries overlap with respect to their domains.

In the present work we follow a different pathway and explore a class of chains that are neither globally symmetric nor disordered and also not locally symmetric in the above

*peter.schmelcher@physnet.uni-hamburg.de

sense of a concatenation of subchains with global symmetries. Our strategy is to generate a chain based on an initial seed that consists of a finite number of elements by the consecutive application of local symmetry operations, namely reflections, according to a given rule. This way a chain is designed that exhibits and is completely covered by a sequence of *overlapping* domains with local symmetries. We demonstrate the plethora of possible evolutionary sequences achievable by the repeated application of local symmetry operations. In general, and starting from the seed sequence, the chain evolves (in space) until it finally, following a finite transient, becomes periodic. We provide a general proof of this behavior which is of constructive character and allows us to predict the transient to periodicity depending on the applied local symmetry transformation. It also yields all relevant quantities such as the final period and the length of the transient. A plethora of transients and resulting periodic behavior can be established this way. In a second step we translate the obtained scheme and chains at hand of specific examples to a tight-binding (TB) Hamiltonian which we subsequently diagonalize. The resulting energy eigenspectrum and eigenstates are then analyzed in some detail. We observe a rich spectral behavior which changes significantly for varying local symmetry transformations. Strong localization and delocalization behavior determined by the presence of local symmetries are detected in the eigenstate properties and are interspersed into series of eigenstates with a smooth energy dependence of their spread.

We proceed as follows. In Sec. II we first introduce our concept of local symmetry operations and dynamics to generate chains with many overlapping domains of local symmetries. We do so by using some representative examples. This allows us already to showcase the existence of a transient and the resulting periodic behavior which vary substantially with varying transformations. A general constructive proof by full induction of the overall behavior of the chains generated by the local symmetry dynamics is provided in the Appendix. In Sec. III we map the previously obtained chains onto a TB Hamiltonian and discuss the resulting energy spectra as well as the so-called eigenstate maps. In Sec. IV we provide our conclusions and an outlook.

II. LOCAL SYMMETRY DYNAMICS-GENERATED CHAINS

This section is dedicated to the introduction of our concept of local symmetry dynamics based on the consecutive application of local symmetry operations in one spatial dimension. After explaining the basics we provide a specific example to gain some intuition with respect to the evolution of the underlying symbolic code including the transient and the final periodic behavior. As a next step we will provide a constructive proof for the general case which allows us to extract the relevant properties and behavior for an arbitrary case.

A. Symbolic code and local symmetry operations: Basic concept and examples

Discrete reflection and translation symmetries are ubiquitous in atomic, molecular and crystalline systems,

respectively. Quasicrystals with their aperiodic order host these symmetries only in a local sense, i.e., only in certain subdomains of the quasiperiodic chain a , for example, reflection symmetry can be found. While there is many such domains in an aperiodic systems with long-range order [9], they are typically disconnected in the sense that they are not generated one from the other. Our starting-point is therefore the idea of creating chains with a large number of local symmetries on overlapping domains based on the repeated application of local symmetry operations. These chains will neither be globally symmetric, i.e., neither reflection symmetric nor periodic, but will exhibit (see below) an evolution of their local symmetries in the course of the multiple application of the local symmetry operations. We call this evolution and approach in the following local symmetry dynamics (LSD). Since this is a general conceptual approach independent of a specific physical platform we will develop it on the level of a symbolic code. Later on (see Sec. III) a concrete realization in the form of a TB Hamiltonian will be investigated.

The key ingredients read as follows. We start from a seed sequence which represents the initial segment of our final symbolic code. Based on this finite seed we apply at the end of it a local reflection operation of n symbols or elements occurring to the left of the position of the corresponding reflection “axis.” Subsequently, we apply another local reflection operation of m symbols at the end of the previously obtained chain. We then repeat this procedure again and again which is encapsulated in the $n : m$ LSD rule. By construction this guarantees that the local symmetries present in the generated chain are strongly overlapping. To get an impression of how such a chain develops and to gain some intuition about the evolution of the corresponding local symmetries we will inspect the case of a series of specific examples, namely $n = 7, m = 1, \dots, 6$ in the following.

Table I shows the evolution of the symbolic code for the above-mentioned cases based on the seed sequence ABCDEFG. $|_k$ indicates the position of the local reflection axis meaning that k chain elements to the left of it are reflected to the right. We observe that in all cases the LSD leads from an initial seed via a transient to a final periodic behavior of the chain. Pictorially speaking the seed undergoes a metamorphosis thereby gradually increasing the degree of the symmetry contained in the chain until it finally becomes periodic. Obviously, the number of different symbols is decreasing along the chain in the course of the evolution to periodicity (see below and the Appendix for quantitative statements along these lines). In this vein the LSD leads to a well-defined loss of information from the seed to the asymptotic behavior of the chain.

Let us discuss the different cases in some more detail. For the cases 7:1, 7:2, and 7:3 the transient consists of only 8, 9, and 10 symbols, respectively; i.e., it is very short. The final unit cell of the periodic sequence is comparatively long amounting to 16, 18, and 20 elements. These unit cells exhibit a plethora of “internal” local symmetries being local reflections and translations. This situation changes when moving on to the cases 7:4, 7:5, and 7:6. Here the transients become substantially longer amounting to 19, 32, and 73 elements, respectively. The final unit cells contain 22, 24, and a single elements. While for the case 7:4 only the A, B, and C elements

TABLE I. The seed of the chain and the local symmetry-generated transients as well as periodic final behavior for specific examples based on the local symmetry dynamics rules 7:1 to 7:6. The abbreviation $|_k$ stands for a reflection operation at the indicated position which reflects k elements of the symbolic code to the left of this position. The underlined sequences represent for each LSD rule the unit cell of the final periodic behavior of the chain.

Seed	ABCDEFG
7:1	$ _7$ G FEDCBA $ _1$ A $ _7$ AABCDEF $ _1$ F $ _7$ F FEDCBA....
7:2	$ _7$ GF EDCBA $ _2$ AB $ _7$ BAABCDE $ _2$ ED $ _7$ DE EDCBA $ _2$ AB $ _7$ BAABCDE....
7:3	$ _7$ GFE DCBA $ _3$ ABC $ _7$ CBAABCD $ _3$ DCB $ _7$ BCD DCBA $ _3$ ABC $ _7$ CBAABCD....
7:4	$ _7$ GFEDCBA $ _4$ ABCD $ _7$ D CBAABC $ _4$ CBAA $ _7$ AABCCBA $ _4$ ABCC $ _7$ C CBAABC....
7:5	$ _7$ GFEDCBA $ _5$ ABCDE $ _7$ EDCBAAB $ _5$ BAABC $ _7$ C BAABBA $ _5$ ABBA $ _7$ AABBAAB $ _5$ BAABB $ _7$ B BAABBA....
7:6	$ _7$ GFEDCBA $ _6$ ABCDEF $ _7$ FEDCBAA $ _6$ AABCDE $ _7$ EDCBAAA $ _6$ AAABCD $ _7$ DCBAAAA $ _6$ AAAABC $ _7$ CBAAAAA $ _6$ AAAAAB $ _7$ B AAAAAA....

are asymptotically present it is only A which occurs finally for the case 7:6. With increasing value of m the number of local symmetries increases for the unit cell of the asymptotically emerging periodic behavior. Having gained an intuition of the “phenomenology” that occurs in case of our specific example, the question arises how representative this behavior is, and whether one can derive and understand the above-mentioned properties in the general case $n:m$ quantitatively. To this end, we provide a proof by explicit construction and full induction in the Appendix. Starting from a general seed this proof provides us with the complete transient behavior for the $n : m$ rule for arbitrary values of n and m and with the corresponding final periodic behavior and unit cell.

Based on the results of the Appendix we can now answer, among others, the following questions. What is the length of the symbolic code, i.e., the number of symbols, until periodicity sets in? Summing up the lengths of the sequences in the transient this amounts to $2(n + mp + m)$ where p is the last branching point index (note that the onset of periodicity is here counted from the corresponding branching points on). If m is of the order of n and consequently p is of the order of m , then the length of the transient is of the order n^2 . Another question concerns the length of the emerging period, i.e., the size of the unit cell. This turns out to simply be $2(n + m)$ in agreement with the above observations. Finally we note that the unit cell of the periodic behavior consists of $n - m$ different symbols out of originally n symbols in the seed. It should be noted that within a series of LSD rules $n:1, \dots, n:(n - 1)$ not every consecutive branch in the tree constituted above in the framework of our proof will be realized.

III. TIGHT-BINDING HAMILTONIAN: SPECTRAL ANALYSIS AND EIGENSTATE MAPS

To explore the properties of the LSD-generated chains derived in Sec. II we use in the following a mapping onto a corresponding TB Hamiltonian. For a discrete chain of length N with sites $\{i|i = 1, \dots, N\}$ we assume that there is only a single value for the off-diagonal couplings C of the nearest neighbors $\langle i, j \rangle$ and the onsite energies D_i follow the LSD chains. This means each symbol of the symbolic code corresponds to a unique value D_i (see below for more details) of this onsite energy on site i . We therefore assume that the

Hamiltonian takes on the following appearance:

$$\mathcal{H} = \sum_{i=1}^N D_i |i\rangle \langle i| + \sum_{\langle i,j \rangle} C |i\rangle \langle j|. \tag{1}$$

In the following subsections we will analyze in some detail the eigenenergy spectrum and the properties of the eigenstates for different LSD chains. Before we enter into a discussion of the corresponding results some remarks are in order concerning the properties of other well-known examples of TB systems. This will allow us to contextualize the results on our LSD chains.

The simplest case of a TB chain refers to the monomer chain AAA... For both open and periodic boundary conditions a single band occurs for the spectrum of the energy eigenvalues. This case can be solved analytically and for periodic boundary conditions (BC) twofold degeneracies are encountered whereas open BCs lead to nondegenerate energy levels. For both cases the eigenstates are delocalized (bulk) states. A chain of dimers ABABAB... results in two bands separated by an energy gap and the periodic case can be solved analytically (see Refs. [21–24] for a corresponding analysis all over). More complicated unit cells and open boundary conditions lead to multiple bands and in particular to the presence of gap energy eigenstates which are localized at the edges of the finite chain and whose number is of the order of the size (number of elements) of the unit cell, depending on how the unit cell is cut off [25,26]. Individual impurities add to this spectrum eigenstates which are exponentially localized [27,28]. The situation becomes richer in terms of symmetries in the case of quasicrystals with their long-range aperiodic order [6–8]. Indeed, the iterative action of a given substitution rule underlying aperiodic lattices lead to a plethora of, e.g., local reflection symmetries or, more precisely, they lead to a quasiperiodic recurrence of reflection symmetries [9] which manifests itself in the corresponding return map. Depending on the spatial complexity of the aperiodic system under consideration, the energy eigenvalues cluster into so-called quasibands and the corresponding eigenstates are neither delocalized all over the bulk nor exponentially localized, but dubbed “critical.” Of particular relevance to the following investigation of TB Hamiltonians based on LSD chains is the local symmetry theory of resonator structures in binary aperiodic chains developed in Ref. [10]. For weak intersite coupling it has

been shown that the eigenstate profile is largely determined by so-called local resonator modes, i.e., eigenmodes confined to locally symmetric domains of the chain. Eigenstates within a given quasiband share the same local resonator modes. Corresponding edge states are then typically localized on locally symmetric domains at the edges of the finite chain.

In the following subsections we will analyze the energy eigenvalue spectrum and the corresponding eigenstates via an eigenstate map for different LSD-generated chains, in analogy to the cases considered in Sec. II A. It is important to note that our focus will be on the evolutionary aspects of the chain including the seed, the transient and the onset of the final periodic steady state. This chain possesses by construction no global symmetries but a plethora of overlapping local symmetries. We will see that the localization properties of the eigenstates are determined and can be controlled by the local symmetry domains.

To be specific we choose the seed $\{A, B, C, D, E, F, G\}$ in Table I and the values of the coefficients $D_i, i = 1, \dots, 7$ in Eq. (1) correspond to $\{1, 2, 3, 4, 5, 6, 7\}$, respectively, whereas the off-diagonal coupling is equal to one. This imprints an intrinsic energy scale into the TB system with a significant, but not too large, contrast $\frac{(D_{i+1}-D_i)}{C}$. Choosing the values for $D_i, i = 1, \dots, 7$ substantially different and having the contrast being of order one, covers the most general case of localization versus delocalization properties of the resulting eigenstates (see discussions below). Later on (see Sec. III D) we will consider also chains with correspondingly smaller contrast, i.e., for stronger off-diagonal couplings. For illustrative reasons our chains consist of the transient including the seed as well as three unit cells of the emerging periodic behavior.

A. 7:1 LSD chain

For this case the transient following the seed consists only of eight chain elements and is followed by a periodic behavior of period 16 with the unit cell FEDCBAAAABCDEFFF (see Table I). Figure 1(a) shows the spectrum of the energy eigenvalues for the 7:1 LSD chain. Clusters of eigenvalues show a plateaulike behavior separated by gaps. There is a few states localized in these energy gaps. This behavior is reminiscent of what could be expected from a finite periodic chain with open boundary conditions.

Let us now analyze the underlying eigenstates and their localization behavior in some detail. The gray scale eigenstate map shown in Fig. 1(b) provides a complete overview of the magnitude of the amplitudes on all sites of the chain for all eigenstates obtained via diagonalization of the Hamiltonian (1). The energetically lowest states 0–2 are predominantly localized on the three locally symmetric AAAA sequences centered around the sites 14/15, 30/31, 46/47 in the chain which correspond to the lowest onsite energies. With increasing degree of excitation these eigenstates become increasingly delocalized but still centered around the corresponding AAAA sequences (see, e.g., states 3–6, 8–13, etc.)

Interdispersed into this rather homogeneous sequence of spatially broadening eigenstates are left-localized (see states 7,13,20) edge states. In the middle of the spectrum the AAAA centered states start to overlap. For higher energies this

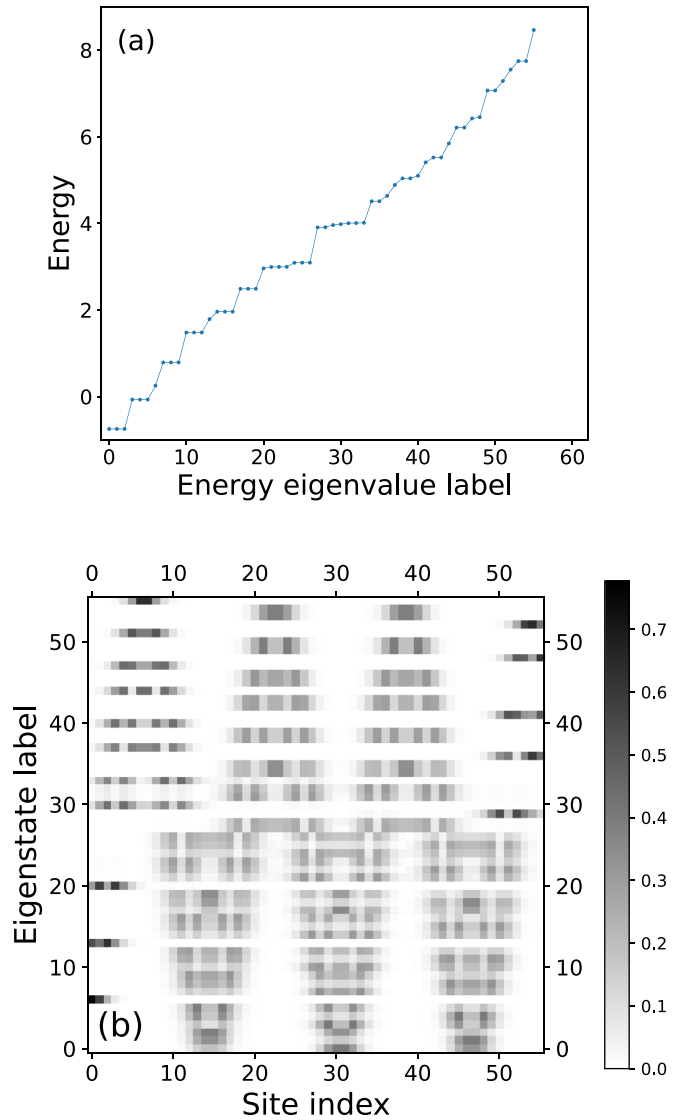


FIG. 1. (a) Spectrum of the energy eigenvalues for a TB chain emerging from a seed ABCDEFG and subsequent application of the 7:1 LSD up to a total of 56 sites, which includes three unit cells of the final periodic behavior. The line is drawn to guide the eye. (b) The corresponding gray scale eigenstate map showing the magnitude of the amplitudes on all sites of the chain for all eigenstates whose labeling 0, ..., 60 is according to an increasing eigenenergy. We use open BCs and the onsite energies corresponding to $\{A, B, C, D, E, F, G\}$ are $\{1, 2, 3, 4, 5, 6, 7\}$, respectively, whereas the off-diagonal coupling is equal to one.

process is inverted and spatially shifted. Now, the eigenstates are centered around the high energy locally symmetric FFFF sequences (sites 22/23, 38/39, 54/55) of the chain and while they are originally rather delocalized they become with increasing degree of excitation more and more focused on the FFFF sequence only. It should be noted that some of these FFFF-centered eigenstates are localized on two and others on a single of these high energy FFFF subdomains. This feature depends on the cutoff of the sequence, i.e., for another cutoff a localization of some of the states on all three and others on only two can be observed. Interdispersed into this

inverted sequence are states 30,33,37,40,44,47,51,55 living on the original seed ABCDEFG and its counterpart which is the first locally reflected sequence GFEDCBA. With increasing degree of excitation this sequence of states becomes increasingly focused around the high energy center GG.

Let us conclude already at this early point of the discussion of our TB analysis with some observations that will equally hold for the following TB setups. The LSD-generated chain exhibits a diversity of different localization properties of their eigenstates which are triggered by two main ingredients. First and foremost the localization is structurally organized by the presence of local symmetries and due to the hierarchy of such symmetries in the chain generated by the LSD rules there is a hierarchy of localization behavior encountered in the eigenstate profiles with increasing energies (see Ref. [10] for a justification and analysis of this property based on degenerate perturbation theory and a corresponding application to quasiperiodic binary chains). This behavior is supported and/or directed by the particular choice of our onsite energies which provides an energetical order for the occupation of the locally symmetric sequences due to the increasing values within the sequence A, ...,G.

B. 7:3 and 7:5 LSD chains

The LSD chain following the 7:3 rule possesses a transient of ten chain elements before it becomes periodic with period 20 and with the unit cell DCBAABCCBAABCCDDCBBCD (see Table I). This unit cell contains now only the symbols A, ...,D, i.e., the high onsite energies according to E, F, G have been removed in the course of the LSD operations. Figure 2(a) shows the spectrum of the energy eigenvalues for the 7:3 LSD chain. Compared to the 7:1 chain of the previous subsection the plateaulike clustering of the energy eigenvalues is attenuated in the central part of the energy eigenvalue spectrum at the cost of an almost linear envelope behavior. For the regimes of low and high energies this plateau behavior is still pronounced. Remarkably, at very high energies a significant enhancement of the spacing among the eigenvalues and consequently of the slope of the spectral eigenvalue curve is observed.

Figure 2(b) shows the eigenstate map for the 7:3 case which defers quite significantly from the corresponding one of the 7:1 case, also from the 7:2 case not shown here. For the lowest energies the eigenstates 0–5 are predominantly localized on the local reflection symmetric BAAB subparts of the chain which are centered around the site pairs 13/14 and 19/20 and repeated after 20 further sites according to the length of the unit cell. The localization centered on the first two pairs 13/14 and 19/20 in the chain possess a slightly higher energy as compared to the following ones due to their tail extending onto the high onsite energies of some of the seed sites. State 6 is a left edge localized state similar to state 24 and 37. States 7 and 8 are localized on the local reflection symmetric CBBC part of the chain involving sites with a higher onsite energy and state 9 is centered on the same sequence but possesses a higher energy due to its position at the right edge. With further increasing degree of excitation the BAAB centered states further delocalize and spread. From state 19 on an energetically broad band of delocalized states appears which

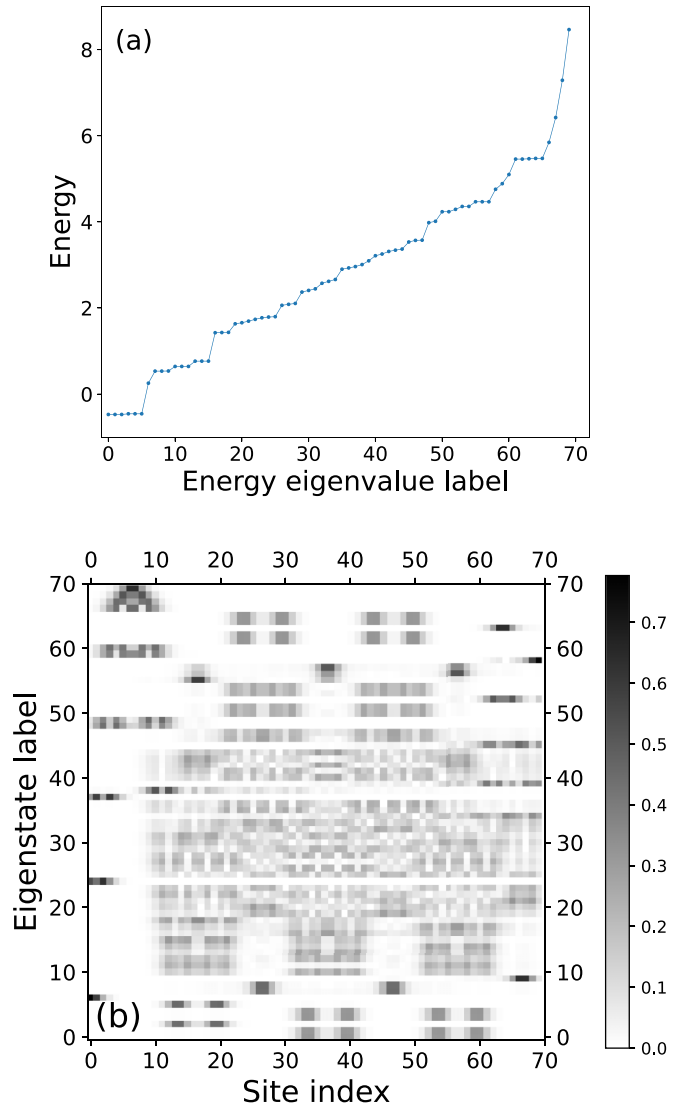


FIG. 2. (a) Spectrum of the energy eigenvalues for a TB chain emerging from a seed ABCDEFG and subsequent application of the 7:3 LSD up to a total of 70 sites, which includes three unit cells of the final periodic behavior. The line is drawn to guide the eye. (b) The corresponding gray scale eigenstate map showing the magnitude of the amplitudes on all sites of the chain for all eigenstates whose labeling 0, ...,69 is according to an increasing eigenenergy. We use open BCs and the onsite energies corresponding to {A,B,C,D,E,F,G} are {1,2,3,4,5,6,7}, respectively, whereas the off-diagonal coupling is equal to one.

resides in particular on the subsequences CBAABCCBAABC possessing also a high degree of local symmetry. States 19 to 23 and 25 to 36 as well as 39 to 45 are completely delocalized on the sequence of the three involved unit cells. For even higher energies eigenstate localization sets in again with a mix of centering around the BCCB, CBBC, and CDDC parts of the chain. On top of this behavior the occupation of the sites of the original seed and its first reflection A, ... G,G, ... A in terms of localized eigenstates appears for the high energy states 48, 49 as well as 59, 60 and finally a series of states 66–69 increasingly narrow down their amplitudes around the center sites GG.

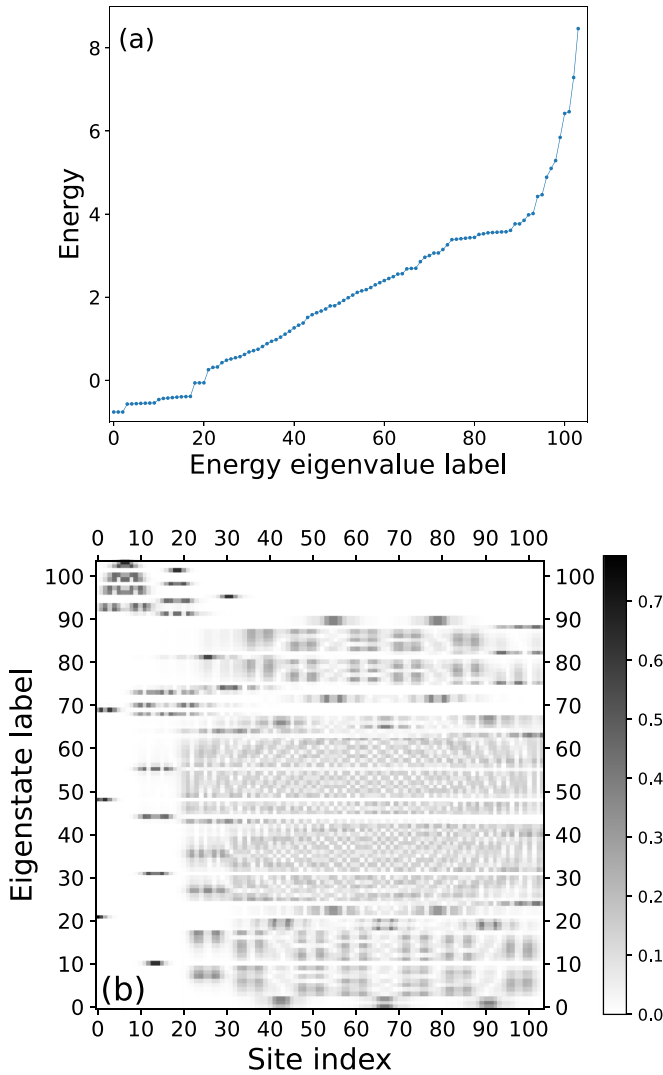


FIG. 3. (a) Spectrum of the energy eigenvalues for a TB chain emerging from a seed ABCDEFG and subsequent application of the 7:5 LSD up to a total of 104 sites, which includes three unit cells of the final periodic behavior. The line is drawn to guide the eye. (b) The corresponding gray scale eigenstate map showing the magnitude of the amplitudes on all sites of the chain for all eigenstates whose labeling 0, ..., 103 is according to an increasing eigenenergy. We use open BCs and the onsite energies corresponding to {A,B,C,D,E,F,G} are {1,2,3,4,5,6,7}, respectively, whereas the off-diagonal coupling is equal to one.

We now analyze the 7:5 LSD chain which possesses a transient of 32 sites before it becomes periodic with period 24 with the unit cell BAABBAABBAAAABBAABBAABBB (see Table I) consisting of two different possibilities for the onsite energies. Figure 3(a) shows the spectrum of the energy eigenvalues for the 7:5 LSD chain. The trend realized in the above discussion of the 7:3 chain continues further, i.e., we have an energetically central part of the spectrum for which an approximately linear envelope behavior can be observed. This linear behavior can be understood by averaging over the onsite energies appearing for the delocalized eigenstates in the center of the spectrum and crudely approximating our chain by a monoatomic one with these averaged tight-binding

values. At low energies the plateau-like clustering still persists. For higher energies we observe an extended plateau before a steep rise of the energies occurs due to an, in part, enhanced energy spacing.

Figure 3(b) shows the eigenstate map for the 7:5 case. Due to the presence of only two onsite energies and the occurrence of multiple locally symmetric sequences such as BAAB, BAAAAB, as well as ABBBBBA subsequences there is a larger portion of delocalized eigenstates observable that however do not populate the original seed sites. Remarkable are also the progression of localized states centered around the sites 13/14 and for high energies centered around the GG and the DEED sequence which increasingly narrow down to their central sites with increasing energy.

C. 7:6 LSD chain

The 7:6 LSD chain possesses a transient of 73 sites before it becomes periodic with period 1 with the unit cell A (see Table I) consisting of only a single possibility for the onsite energies. Figure 4(a) shows the spectrum of the energy eigenvalues for the 7:6 LSD chain. Compared to the previous cases an approximately linear envelope behavior is now present also for the low energies and for high energies a smooth nonlinear upward behavior is observed.

The resulting eigenstate map in Fig. 4(b) shows several series of localized eigenstates in a progressive manner in the low to intermediate energy regime. This is a remarkable localization behavior and happens at the cost of few delocalized states as compared to the previously discussed cases 7 : x, x = 1, 3, 5. The origin of these unexpected localization features are again the locally reflection symmetric sequences occurring in the chain, but now they come along with a certain transient scaling behavior. This means that along the chain (see Table I) we encounter now the subsequences B(A)₂B, B(A)₄B, B(A)₆B, B(A)₈B, and B(A)₁₀B centered around the sites 13/14, 26/27, 39/40, 52/53, and 65/66, respectively. Here (A)_n stands for an n-fold repeated symbol A. Naturally, the width of these localized eigenstates increases with increasing number of sites involved in the above-mentioned sequences B(A)_nB. In the high energy regime another several series of localized eigenstates appear which are now centered and localized on the sequences FGGF, EFFE, DEED, CDDC, and BCCB with decreasing energy. Their widths are comparable as can be observed in Fig. 4(b).

D. LSD chains with stronger off-diagonal couplings

Let us finally explore the case of an enhanced off-diagonal coupling strength C = 5. Figure 5 shows the eigenstate map for the TB chain for such a strong coupling for the cases of an (a) 7:1 and (b) 7:6 LSD rule. Compared to the case of a weaker coupling discussed in the previous subsections we observe now an energetically broad band for intermediate energies for which the eigenstates are delocalized over the complete chain, including the initial seed of the chain. For some comparatively narrow regions of high and low energies series of localized eigenstates appear whose amplitudes are centered around the locally symmetric subparts of the chains, as discussed above. The broadening (for low energies), respectively, narrowing

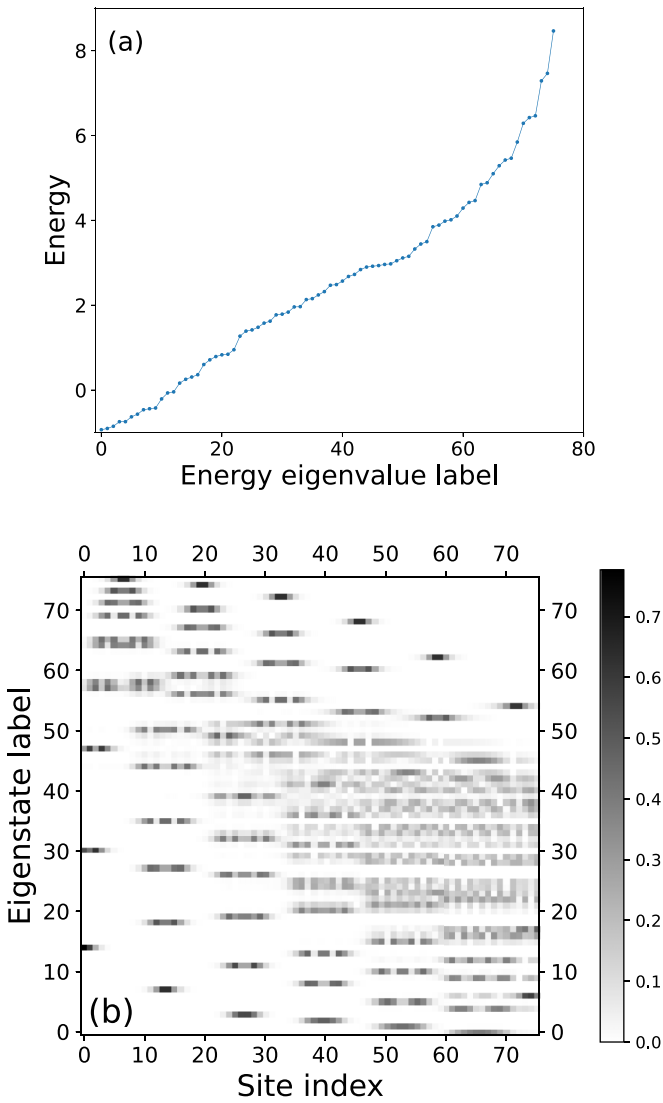


FIG. 4. (a) Spectrum of the energy eigenvalues for a TB chain emerging from a seed ABCDEFG and subsequent application of the 7:6 LSD up to a total of 76 sites, which includes three unit cells of the final periodic behavior. The line is drawn to guide the eye. (b) The corresponding gray scale eigenstate map showing the magnitude of the amplitudes on all sites of the chain for all eigenstates whose labeling 0, ...,75 is according to an increasing eigenenergy. We use open BCs and the onsite energies corresponding to {A,B,C,D,E,F,G} are {1,2,3,4,5,6,7}, respectively, whereas the off-diagonal coupling is equal to one.

(for high energies) of the localization of the eigenstates with increasing degree of excitation can also be observed here. In Fig. 5(b) there is a series of domain localized eigenstates 0–4 that possess a small but finite overlap and therefore covers, apart from the initial seed, the complete chain. Similarly there is a series of slightly overlapping eigenstates in the high energy regime that cover the complete chain.

IV. CONCLUSIONS AND OUTLOOK

The present work addresses a class of systems, specifically one-dimensional chains, which fall into the gap between

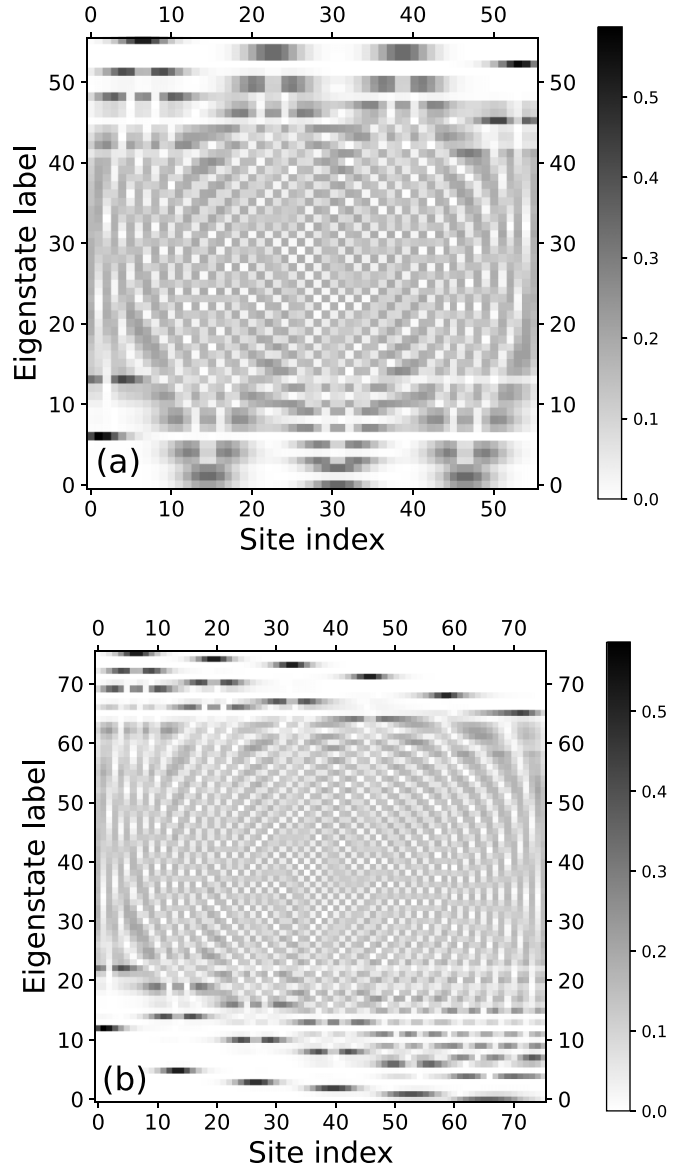


FIG. 5. (a) Gray scale eigenstate map for a TB chain with strong coupling $C = 5$ emerging from a seed ABCDEFG and subsequent application of the (a) 7:1 LSD up to a total of 56 sites, which includes three unit cells of the final periodic behavior. (b) The same as in panel (a) but for the 7:6 LSD chain up to 76 sites. We use open BCs and the onsite energies corresponding to {A,B,C,D,E,F,G} are {1,2,3,4,5,6,7}, respectively.

highly ordered periodic crystals as well as quasicrystals with aperiodic long-range order and disordered chains. On an abstract level, they are constituted from a symbolic seed sequence by the repeated application of local reflection operations following certain rules. We have been here focusing on the class of rules $n:m$ which state that the local reflection operations involve n and m symbols in an alternating periodic manner. A study of a few example cases showed us that the repeated application of the local reflection operation provides us, starting from the seed, with a remarkable evolutionary behavior in the form of a transient finally providing a periodic steady state. Our focus in this work is on this evolutionary

The base case for the proof by induction:

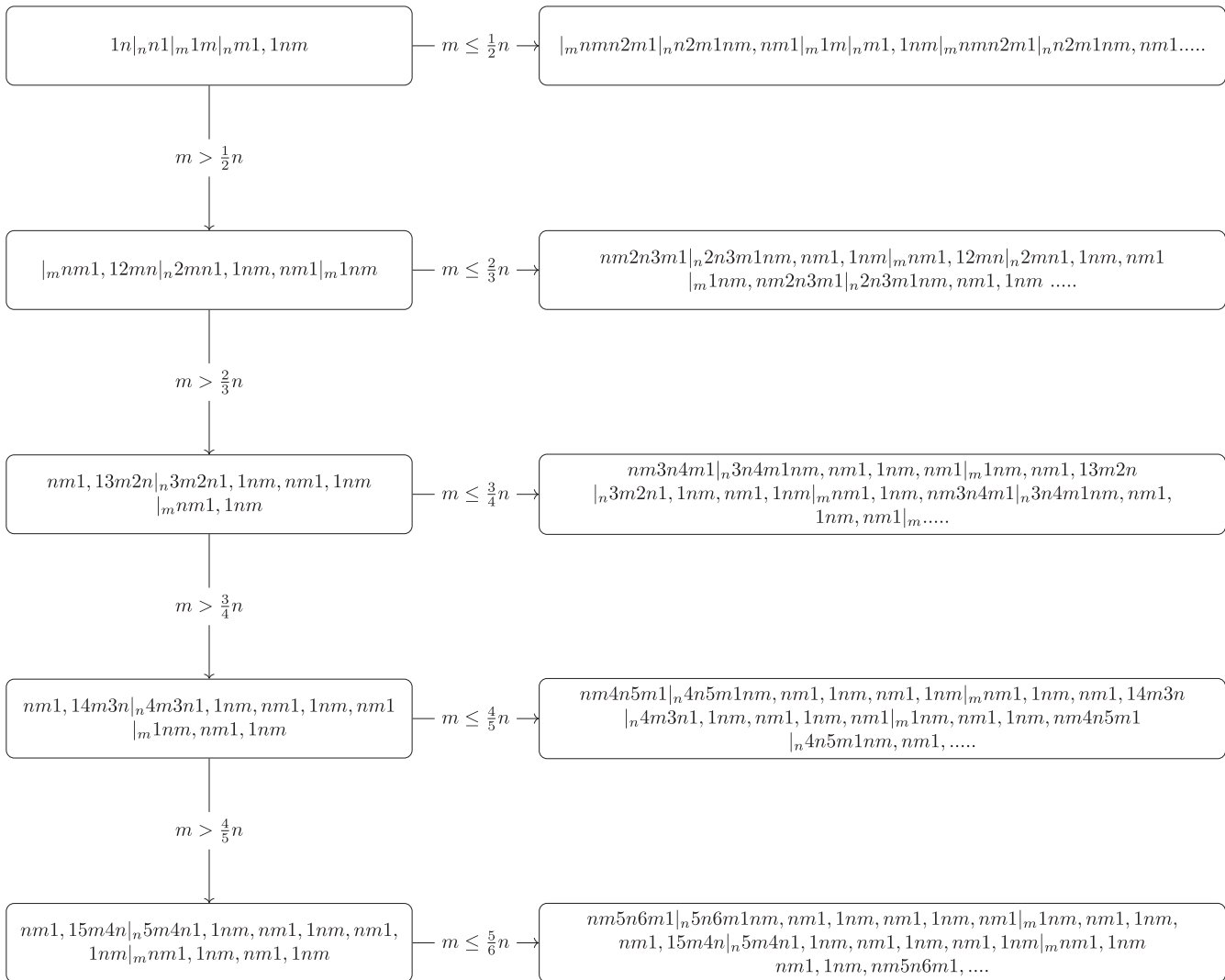


FIG. 6. The initial steps for the proof by induction. The initial seed is contained in the uppermost left rounded box. The flowchart shows (i) the pathway to periodic behavior along the horizontal branches and (ii) the pathway to higher values of m passing along the vertical branching sequences. A branching occurs for each case $m = \frac{p}{n}$, $p = 1, 2, \dots$. Abbreviations are: $1n = \{1, \dots, n\}$, $n1 = \{n, \dots, 1\}$, $1nm = \{1, \dots, n - m\}$, $nm1 = \{n - m, \dots, 1\}$, $1m = \{1, \dots, m\}$, $m1 = \{m, \dots, 1\}$, $12mn = \{1, \dots, (2m - n)\}$, $2mn1 = \{(2m - n), \dots, 1\}$ and more generally $nmpn(p + 1)m1 = \{(n - m), \dots, (pn - (p + 1)m + 1)\}$. $|_n$ indicates a local reflection operation of n symbols.

behavior followed by the onset of the steady state. The content, i.e., appearance of the resulting unit cell largely varies with the rules $n:m$. We have provided a general proof of this behavior thereby understanding the variability of the pathway to periodicity and its final appearance. As a consequence, and due to the constructive character of the proof, we could predict the complete evolution of the chain up to the onset of the periodic steady state. We obtained thereby the final period, the final number of independent chain elements and the overall appearance of the unit cell. This appearance is composed of an inhomogeneous alternating series of subchains with local symmetries, and of varying length and recursively defined content.

As a consequence of the construction principle of the chain it contains a large number of local reflection and

translation symmetries that strongly overlap and repeat in different shapes and content. Opposite to, e.g., the substitution rules generating aperiodic long-range ordered chains our local symmetry dynamics rule leaves intact the chain of a certain generation while building up the next one. The strong impact of the presence of these multiple and nested local symmetries on the properties of such a chain became very clear in the second part of this investigation. We mapped the symbolic code onto a tight-binding Hamiltonian where the onsite energies follow the chains symbolic sequence in the form of corresponding numerical values. In the course of a corresponding spectral analysis, including the behavior of the energy eigenvalues and the eigenstates, a rich variability could be observed. Specifically the localization properties of the eigenstates changed from series of localized

The p to $p + 1$ induction step for the proof by induction:

This is divided into several cases:

First case: p even and $\frac{p}{p+1}n \geq m > \frac{p-1}{p}n$.

$$nm1|_m \underbrace{1nm, \dots, 1nm}_{(p-1)} nmpn(p+1)m1|_n pn(p+1)m1nm, \underbrace{nm1, \dots, nm1}_{(p-1)} 1nm|_m \underbrace{nm1, \dots, nm1}_{(p-1)} 1pm(p-1)n|_n pm(p-1)n1, \underbrace{1nm, \dots, 1nm}_{(p-1)} nm1|_m \underbrace{1nm, \dots, 1nm, nmpn(p+1)m1|_n pn(p+1)m1nm, \dots}_{(p-1)}$$

which establishes periodicity.

Second case: p even and $m > \frac{p}{p+1}n$.

$$nm1|_m \underbrace{1nm, \dots, 1nm}_{(p-1)} nm1, 1(p+1)m|_n pn(p+1)m|_n pm1, 1nm, \underbrace{nm1, \dots, nm1}_{(p-1)} 1nm|_m nm1, \underbrace{1nm, \dots, 1nm}_{(p-1)} \begin{cases} nm(p+1)n(p+2)m1 & \text{if } m \leq \frac{p+1}{p+2}n \\ nm1, 1(p+2)m(p+1)n & \text{if } m > \frac{p+1}{p+2}n \end{cases}$$

which completes the induction step for the second case.

Third case: p odd and $\frac{p}{p+1}n \geq m > \frac{p-1}{p}n$.

$$1nm|_m \underbrace{nm1, \dots, 1nm}_{(p-1)} nmpn(p+1)m1|_n pn(p+1)m1nm, \underbrace{nm1, \dots, 1nm}_{(p-1)} nm1|_m \underbrace{1nm, \dots, nm1}_{(p-1)} 1pm(p-1)n|_n pm(p-1)n1, \underbrace{1nm, \dots, nm1}_{(p-1)} 1nm|_m \underbrace{nm1, \dots, 1nm, nmpn(p+1)m1|_n pn(p+1)m1nm, \underbrace{nm1, \dots, 1nm}_{(p-1)} nm1, \dots}_{(p-1)}$$

which establishes periodicity.

Fourth case: p odd and $m > \frac{p}{p+1}n$.

$$1nm|_m \underbrace{nm1, \dots, 1nm}_{(p-1)} nm1, 1(p+1)m|_n pn(p+1)m|_n pm1, 1nm, \underbrace{nm1, \dots, 1nm}_{(p-1)} nm1|_m 1nm, \underbrace{nm1, \dots, 1nm}_{(p-1)} \begin{cases} nm(p+1)n(p+2)m1 & \text{if } m \leq \frac{p+1}{p+2}n \\ nm1, 1(p+2)m(p+1)n & \text{if } m > \frac{p+1}{p+2}n \end{cases}$$

which completes the induction step for the fourth case.

FIG. 7. The p to $p + 1$ induction step for the proof involving all possible branchings, i.e., cases. Notation is the same as described in the caption of Fig. 6.

eigenstates whose localization centers are determined by the locally reflection symmetric subchains to delocalized states sometimes in a continuous and sometimes in a more abrupt manner with varying excitation energy. Our analysis clearly demonstrates that local and in particular overlapping local symmetries provide a powerful means to control the centering and spreading of eigenstates. Certain locally symmetric domains act as a nucleus for the increased spreading of localized eigenstates with increasing degree of excitation whereas others show a corresponding inverted behavior. Depending on the assigned onsite values to the domains and their couplings they appear in the low or high energy regime with a band of delocalized eigenstates separating them. This opens the pathway of a systematic design of the localization of the eigenstates individually and with respect to each other by the sophisticated use of the overlapping local symmetry domains.

While we have been focusing in the present work on a specific class of local symmetry operations that generate the chain there is many other possibilities and open questions to be addressed in the future. Reaching beyond the $n:m$ rule

can be imagined in many different ways. One problem is the roadmap to periodicity: under what conditions does periodicity occur and if not, what are the possible asymptotic behaviours passing the transient phase? Is there new classes of order that possibly emerge via local symmetry dynamics-generated chains and what would be their spectral or even topological properties? These, and related questions, are left to future investigations.

Finally, let us briefly address the question of an experimental realization of the spectral properties of our local symmetry-generated chains. An all optical realization of our tight-binding systems can be achieved in the framework of (integrated) coupled photonic waveguide lattices [29,30]. The fabrication and characterization is possible by femtosecond lasers that controllably change the materials molecular structure and consequently lead to a spatially varying refraction index. The coupling is here constituted by evanescent light fields between neighboring wave guides. Such a photonic realization would only allow to explore setups with a limited number of wave guides, i.e., a finite tight-binding lattice.

ACKNOWLEDGMENTS

The author acknowledges discussions with F. K. Diakonos, M. Röntgen, and M. Pyzh. This work is supported by the Cluster of Excellence “Advanced Imaging of Matter” of the Deutsche Forschungsgemeinschaft (DFG)-EXC 2056, Project ID No. 390715994.

APPENDIX: PROOF OF $n:m$ LOCAL SYMMETRY DYNAMICS

We provide in this Appendix a constructive proof by induction of the symbolic sequence generated by a general $n:m$ LSD where we always assume that $n > m$. To this end it is advisable and instructive to employ as an encoding of the elements of the chain not the alphabetical letters used in the previous Sec. II A but a numerical encoding. Specifically this means that the initial seed ABCD... is now replaced by the symbolic sequence $1, \dots, n$ if n seed elements are present (please note here the double use of n ; first as a symbolic variable and second as a number). This way of encoding facilitates the local symmetry operations in the course of the LSD substantially and adds to the transparency of the below-given proof in Figs. 6 and 7, respectively. The numbers used here are therefore unique placeholders for a corresponding symbol. The hereby used notation is as follows: $1n = \{1, \dots, n\}$, $1nm = \{1, \dots, n - m\}$, $1m = \{1, \dots, m\}$, $12mn = \{1, \dots, (2m - n)\}$, and more generally $nm pn(p + 1)m1 = \{(n - m), \dots, (pn - (p + 1)m + 1)\}$. $|_n$, as mentioned already above, indicates a local reflection operation on n symbols.

To start the proof by full induction one has to perform some first steps. We will here for reasons of illustration of the concept and overall flow of the general case provide a few more initial steps as absolutely necessary for the proof. Figure 6 shows a flowchart of the first few steps and branching sequences. The flowchart consists of horizontal and vertical flows which emerge at every branching point $m = \frac{1}{2}n, \frac{2}{3}n, \frac{3}{4}n, \frac{4}{5}n$. Following the corresponding horizontal branches for $m \leq \frac{1}{2}n, \frac{2}{3}n, \frac{3}{4}n, \frac{4}{5}n$ leads to periodicity with different characteristic unit cells which can be read off from the right-hand-side boxes in Fig. 6. In case m larger than a given ratio one proceeds along the vertical direction of the flowchart until, finally, the horizontal case has to be chosen, which leads to periodicity. Already from these initial steps it is evident that both the transient as well as the final unit cell are composed of $1nm, nm pn(p + 1)m1 = \{(n - m), \dots, (pn - (p + 1)m + 1)\} | p \in \mathbb{N}$ and $1(p + 1)m pn = \{(1, \dots, ((p + 1)m - pn))\}$ as well as their inverted sequences. The increasing length of the transient as well as the size of the final unit cell with increasing ratio $\frac{m}{n}$, $m, n \in \mathbb{N}$ is evident from these initial steps already.

In Fig. 7 the p to $p + 1$ induction step is performed. The various cases are explicitly mapped out and the route to periodicity (horizontal branches in Fig. 6) as well as the extension of the transient (vertical branch in Fig. 7) up to the next branching point are shown. In this p th step sequences of $1nm$ (respectively, $nm1$) appear in a p -fold manner intermingled with elements of the structure $nm pn(p + 1)m1, 1(p + 1)m pn$. This concludes the proof by explicit construction and provides us with the content of the transient and the final unit cell.

-
- [1] M. Hamermesh, *Group Theory and its Applications to Physical Problems*, Dover Books on Physics and Chemistry (Dover Books, Mineola, NY, 1962).
- [2] J. F. Cornwell, *Group Theory in Physics* (Academic Press, San Diego, CA, 1984).
- [3] H. Friedrich, *Theoretical Atomic Physics*, 4th ed. (Springer International Publishing AG, Berlin, 2017).
- [4] P. R. Bunker, *Molecular Symmetry and Spectroscopy* (Academic Press, San Diego, CA, 1979).
- [5] S. M. Girvin and K. Yang, *Modern Condensed Matter Physics* (Cambridge University Press, Cambridge, UK, 2019).
- [6] D. Levine and P. J. Steinhardt, Quasicrystals: A new class of ordered structures, *Phys. Rev. Lett.* **53**, 2477 (1984).
- [7] D. Shechtman, I. Blech, D. Gratias, and J. W. Cahn, Metallic phase with long-range orientational order and no translational symmetry, *Phys. Rev. Lett.* **53**, 1951 (1984).
- [8] J. B. Suck, M. Schreiber, and P. Häussler, *Quasicrystals: An Introduction to Structure, Physical Properties and Applications* (Springer Science & Business Media, Berlin, 2002).
- [9] C. Morfonios, P. Schmelcher, P. A. Kalozoumis, and F. K. Diakonos, Local symmetry dynamics in one-dimensional aperiodic lattices: A numerical study, *Nonlin. Dyn.* **78**, 71 (2014).
- [10] M. Röntgen, C. V. Morfonios, R. Wang, L. Dal Negro, and P. Schmelcher, Local symmetry theory of resonator structures for the real-space control of edge states in binary aperiodic chains, *Phys. Rev. B* **99**, 214201 (2019).
- [11] E. Maciá, The role of aperiodic order in science and technology, *Rep. Prog. Phys.* **69**, 397 (2006).
- [12] E. Maciá, Exploiting aperiodic designs in nanophotonic devices, *Rep. Prog. Phys.* **75**, 036502 (2012).
- [13] P. A. Kalozoumis, C. Morfonios, F. K. Diakonos, and P. Schmelcher, Invariants of broken discrete symmetries, *Phys. Rev. Lett.* **113**, 050403 (2014).
- [14] P. A. Kalozoumis, O. Richoux, F. K. Diakonos, G. Theocharis, and P. Schmelcher, Invariant currents in lossy acoustic waveguides with complete local symmetry, *Phys. Rev. B* **92**, 014303 (2015).
- [15] N. Schmitt, S. Weimann, C. V. Morfonios, M. Röntgen, M. Heinrich, P. Schmelcher, and A. Szameit, Observation of local symmetry in photonic systems, *Laser Photon. Rev.* **14**, 1900222 (2020).
- [16] P. A. Kalozoumis, C. Morfonios, F. K. Diakonos, and P. Schmelcher, Local symmetries in one-dimensional quantum scattering, *Phys. Rev. A* **87**, 032113 (2013); P. A. Kalozoumis, C. Morfonios, N. Palaiodimopoulos, F. K. Diakonos, and P. Schmelcher, Local symmetries and perfect transmission in aperiodic photonic multilayers, *ibid.* **88**, 033857 (2013).
- [17] C. Morfonios, P. A. Kalozoumis, F. K. Diakonos, and P. Schmelcher, Nonlocal discrete continuity and invariant currents in locally symmetric effective Schrödinger arrays, *Ann. Phys.* **385**, 623 (2017).

- [18] P. Schmelcher, S. Krönke, and F. K. Diakonou, Dynamics of local symmetry correlators for interacting many-particle systems, *J. Chem. Phys.* **146**, 044116 (2017).
- [19] V. E. Zampetakis, M. K. Diakonou, P. A. Kalozoumis, F. K. Diakonou, and P. Schmelcher, Invariant current approach to wave propagation in locally symmetric structures, *J. Phys. A* **49**, 195304 (2016).
- [20] C. V. Morfonios, M. Röntgen, F. K. Diakonou, and P. Schmelcher, Transfer efficiency enhancement and eigenstate properties in locally symmetric disordered finite chains, *Ann. Phys.* **418**, 168163 (2020).
- [21] C. M. Goringe, D. R. Bowler, and E. Hernández, Tight-binding modelling of materials, *Rep. Prog. Phys.* **60**, 1447 (1997).
- [22] S. Kouachi, Eigenvalues and eigenvectors of tridiagonal matrices, *Electron. J. Lin. Alg.* **15**, 115 (2006).
- [23] D. Kulkarni, D. Schmidt, and S.-K. Tsui, Eigenvalues of tridiagonal pseudo-Toeplitz matrices, *Lin. Alg. Appl.* **297**, 63 (1999).
- [24] A. R. Willms, Analytic results for the eigenvalues of certain tridiagonal matrices, *SIAM J. Matrix Anal. Appl.* **30**, 639 (2008).
- [25] J. Zak, Symmetry criterion for surface states in solids, *Phys. Rev. B* **32**, 2218 (1985).
- [26] T. Fukui, Theory of edge states based on the Hermiticity of tight-binding Hamiltonian operators, *Phys. Rev. Res.* **2**, 043136 (2020).
- [27] D. J. Thouless, Electrons in disordered systems and the theory of localization, *Phys. Rep.* **13**, 93 (1974).
- [28] T. Brandes and S. Kettmann, *The Anderson Transition and Its Ramifications Localisation, Quantum Interference, and Interactions, Lecture Notes in Physics* (Springer-Verlag, Berlin, 2003).
- [29] A. Szameit and S. Nolte, Discrete optics in femtosecond-laser-written photonic structures, *J. Phys. B: At. Mol. Opt. Phys.* **43**, 163001 (2010).
- [30] M. Gräfe and A. Szameit, Integrated photonic quantum walks, *J. Phys. B* **53**, 073001 (2020).